AgileDARN Radar Echo Automatic Classification Algorithm Using Support Vector Machine

Guangming Li[1, 2, *]

Abstract—In this paper, an AgileDARN (Agile Dual Auroral Radar Network) radar echo classification method based on support vector machine is proposed. AgileDARN radar echo includes ionospheric backscattering echo, meteor echo, noise interference, etc. With the continuous operation of AgileDARN radar, the amount of data increases rapidly, requiring efficient and reliable classification methods. In order to efficiently classify the echoes of AgileDARN radar, this paper proposes an echo classification method based on support vector machine. By analyzing the characteristics of the autocorrelation function (ACF) of the sampled data and extracting the features, the support vector machine (SVM) classification method is adopted to classify AgileDARN echo into ionospheric backscattering echo, meteor echo, and noise interference. The data analysis shows that the classification accuracy of training data set is more than 99%, and that of test data set is more than 95%. Using this classification model to classify 1800 echo data of AgileDARN radar, the classification accuracy is more than 91% compared with the result of manual interpretation.

1. INTRODUCTION

The AgileDARN radar is a new generation SuperDARN radar with an all-digital design. SuperDARN radars are widely distributed in the northern and southern hemispheres for ionospheric plasma and irregularities detection [1]. AgileDARN radar, like SuperDARN radars, operates at high frequency bands of 8–20 MHz, emits multi-pulses, and obtains backscattering echoes from plasma and irregulars in the ionosphere [2, 3]. Echo signals received by AgileDARN radar mainly include ionospheric backscattering echo, meteor echo, various noise interference echo, etc. [4–7]. Ionospheric backscattering echo is mainly the backscattering of plasma and irregularities in the ionosphere, and it can be used to study ionospheric convection, ionospheric and magnetospheric coupling, and other space science problems [1]. Meteor echo is the echo formed by radar signal reflected by ionized wake formed by meteoroid entering the earth's atmosphere. Meteor trials are driven by atmospheric neutral wind and drifts; therefore, meteor echo can be used to invert atmospheric neutral wind and further study scientific problems such as tides and planetary waves [8, 9]. All kinds of noise interference are useless signals received by AgileDARN radar and need to be removed. It can be seen from the above analysis that the classification of AgileDARN radar echo is of great significance for subsequent research. For the convenience of discussion, the ionospheric backscattering echo is called the ionospheric echo, and all the echoes except the ionospheric echo and meteor echo are called noise.

Many previous studies on SuperDARN radar echo classification have been done. For ionospheric echo classification, Baker et al. proposed a classification method for ionospheric echoes based on doppler velocity and spectral width, and considered the echoes with doppler velocity greater than 30 m/s and spectral width greater than 35 m/s as ionospheric echoes [10, 11]. Andre et al. proposed a

* Corresponding author: Guangming Li (liguangming627@163.com).
[1] State key Laboratory of Space Weather, National Space Science Center, Chinese Academy of Sciences, Beijing 100190, China.
[2] University of Chinese Academy of Sciences, Beijing 100049, China.

SuperDARN radar echo classification method based on spectral width, ACF phase deviation, and power deviation based on autocorrelation data of SuperDARN radar echo [12]. Blanchard et al. proposed a method of extracting ionospheric echoes using doppler velocity and spectral width combined with probability density function [13]. In addition, many scholars have carried out ionospheric classification of SuperDARN radar echo by using longer multi-pulse sequences [14], developing higher-precision spectral analysis methods [15], using ray tracing technology [16], analyzing complex signals in the scattering region [17], and analyzing the amplitude and phase of multi-pulse signals [18]. Meteor echoes were first discovered by Hall et al. in SuperDARN radar echoes [7]. Since then, many scholars have carried out research on meteor echo extraction algorithms based on SuperDARN radar. Hussey et al. proposed a method of extracting meteor echoes based on doppler features [7, 8, 19]. Tsutsumi et al. presented the method of raw time series analysis to detect meteor echo [20, 21]. Parris put forward a modification of the SuperDARN radar hardware to use digital receiver with flexible filtering, then, the meteor echo is extracted by time profile [22]. The above ionospheric and meteor echo extraction methods can be used effectively to extract ionospheric and meteor echoes from SuperDARN; however, both are time-consuming work even for experts in the field. For the continuous operation of AgileDARN radar, the amount of data is constantly increasing, so more reliable and efficient data classification methods need to be considered.

In order to achieve efficient and automatic classification of AgileDARN radar echo, this paper proposes an echo classification method based on support vector machine (SVM). Firstly, the Autocorrelation Functions (ACF) of each beam and each range gate are obtained by calculating the Autocorrelation of IQ data sampled by radar; secondly, the characteristics of ACF of meteor echo, ionospheric echo, and noise are analyzed, and the characteristics of each echo are extracted. The data are divided into training data set and testing data set, and then, the training data set is used to train the SVM to get the classification model. The testing data set is used to generalize the model. Finally, the classification model is used to classify the data of AgileDARN radar.

The rest of the paper is organized as follows. Section 2 analyzes the calculation method of ACF and discusses the characteristics of the ACF of meteor echo, ionospheric echo, and noise. Section 3 discusses the classification method based on SVM and gives the classification results. Finally, the paper is summarized.

2. ACF CHARACTERISTICS OF AGILEDARN ECHO

2.1. Calculation Method of ACF

AgileDARN radar is a digital phased array radar, comprising two Twin Terminated Folded Dipole (TTFD) antenna arrays. The main array is a linear array composed of 16 antennas, which has the ability of transmitting and receiving, and the interferometer array is a linear array composed of 4 antennas with receiving capability only. The main array can generate 24 beams through beam synthesis, covering a field of view of $78°$, and each beam is composed of 75 slant range gates. The maximum detection range can be $3555\,\text{km}$. AgileDARN radar transmits pulse signals and samples the echo signals to obtain orthogonal IQ data, and through autocorrelation calculation, the autocorrelation function (ACF) of each beam of each slant range gate can be obtained [23, 24]. Doppler velocity, spectral width, and backscattering power can be calculated by fitting the ACF [3].

Assuming that the g sampling voltage of the radar receiver at time t is V, then

$$V(t, g) = I(t, g) + iQ(t, g) \tag{1}$$

where I represents the real part of receiver sampling, and Q represents the imaginary part of receiver sampling. AgileDARN radar periodically emits multi-pulse sequences, which are unequally separated in time by integer times of the basic delay interval, so the ACF is

$$R(\tau, g) = V(t, g) V^*(t + k\tau_0, g) \tag{2}$$

where τ_0 stands for the basic delay interval, k the delay number, τ the delay time, and asterisk the complex conjugate.

AgileDARN radar usually emits multiple multi-pulse sequences to improve the signal-to-noise ratio, and the average ACF can be obtained by averaging multiple pairs of sampled complex voltage values

$$\tilde{R}(\tau, g) = \frac{1}{N} \sum_{n=1}^{N} V(t, g) V^*(t + k\tau_0, g) \tag{3}$$

where N represents the number of multi-pulse sequences transmitted. The amplitude and phase of the ACF can be obtained from Equations (4) and (5):

$$A(\tau, g) = \sqrt{\tilde{R}_I^2(\tau, g) + \tilde{R}_R^2(\tau, g)} \tag{4}$$

$$\phi(\tau, g) = \frac{\tilde{R}_I(\tau, g)}{\tilde{R}_R(\tau, g)} \tag{5}$$

In this formula, $\tilde{R}_R(\cdot)$ refers to the real part of the ACF, and $\tilde{R}_I(\cdot)$ refers to the imaginary part of the ACF. It can be seen from Equations (4) and (5) that the amplitude and phase of the ACF can be determined by the real and imaginary parts of the ACF.

When AgileDARN radar is observing the ionosphere, the signal emitted by the radar is a typical 8 pulse sequence unequally spaced [2]; pulse width is $300\,\mu s$; the basic delay interval is $\tau_0 = 1500\,\mu s$; lag $k = 23$; and slant range gates $G = 75$ after autocorrelation calculation. All of the IQ data sampled by AgileDARN radar are calculated by autocorrelation to obtain $\tilde{R}(\tau)$.

2.2. ACF Characteristics of Ionospheric Echo

Figure 1 shows the real and imaginary parts, amplitude and phase of a typical ionospheric echo mean ACF [25]. As can be seen from Figure 1(a), the real part of the ACF has a maximum value at zero lag, and the imaginary part of ACF is zero at zero lag. Both real and imaginary parts decay in amplitude with increasing lag. Figure 1(b) shows the amplitude of the ACF, which attenuates with the increase of the lag, exponential fitting or Gaussian fitting is generally selected for the amplitude fitting [26]. Figure 1(c) shows the phase of the ACF without unwrapping.
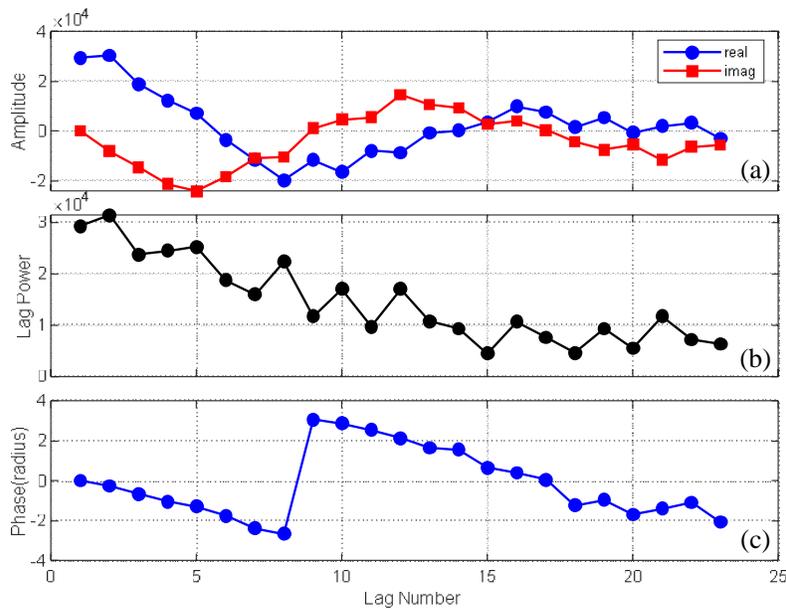

Figure 1. Characteristics of ACF of ionospheric echo.

2.3. ACF Characteristics of Meteor Echo

The meteor echo is usually in the near slant range of the AgileDARN, usually within 400 km [7]. The initial sampling distance of AgileDARN radar during ionospheric observation is 180 km, and each slant range gate is 45 km. Five range gates correspond to a distance of 405 km; therefore, the echo data in the 5 range gates is selected during meteor echo screening. Figure 2 shows the power characteristics of meteor echo, corresponding to the 4th range gate with slant range of 360 km. It can be seen from the figure that the power of meteor echo gradually increases. Figure 3 shows the characteristics of the ACF of the meteor echo in Figure 2. Figure 3(a) shows the real and imaginary features of the meteor echo ACF. Figure 3(b) shows the amplitude characteristics of meteor echo ACF. Figure 3(c) shows the phase characteristics of the ACF of meteor echo, which shows a trend of linear change.
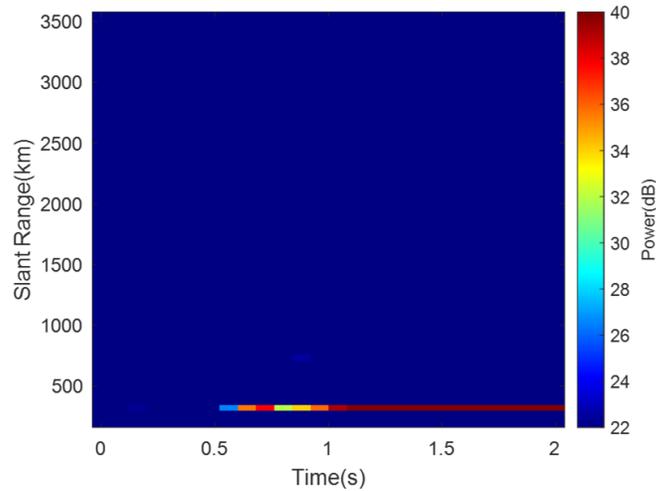

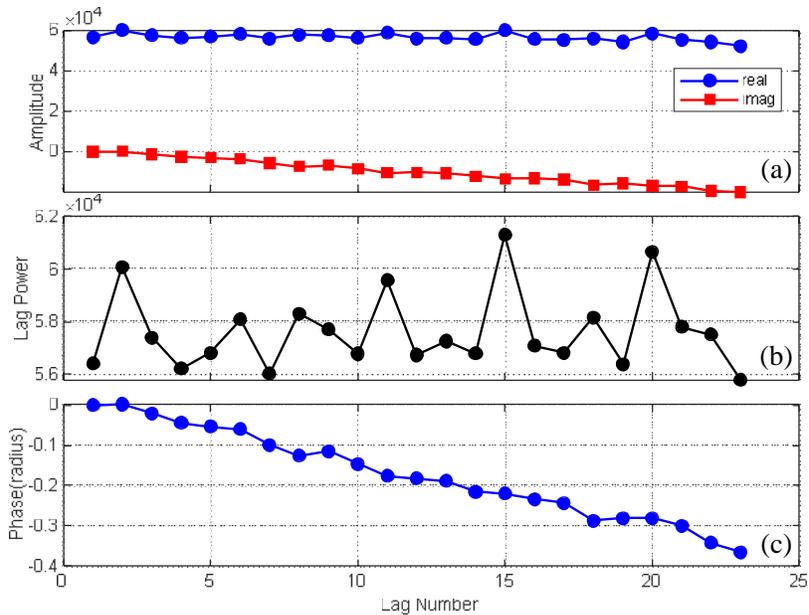**Figure 2.** Characteristics of meteor echo power.

Figure 3. ACF characteristics of meteor echo.

2.4. Feature Extraction of ACF

Sections 2.2 and 2.3 analyze the characteristics of the ACF of ionospheric echo and meteor echo, from which it can be seen that the real and imaginary parts of the ACF of ionospheric echo are cosine oscillation attenuation and sinusoidal oscillation attenuation. The real and imaginary parts of the meteor echo ACF attenuate linearly. The echo whose ACF does not satisfy these two variation trends is noise. It can be seen from Equations (4) and (5) that the amplitude and phase of radar echo can be calculated by the real and imaginary parts of the ACF; therefore, the real and imaginary parts of the ACF can determine whether the echo of AgileDARN radar is ionospheric echo, meteor echo, or noise. Figure 4 shows the real and imaginary characteristics of the ACF of typical ionospheric echoes, meteor echoes, and noise. Figures 4(a1), (a2), (a3) show the characteristics of the real and imaginary parts of the ionospheric echo. It can be seen from the figure that although some points deviate, the overall trend is still cosine oscillation attenuation and sinusoidal oscillation attenuation. Figures 4(b1), (b2), (b3) show the characteristics of the real and imaginary parts of meteor echo. Figures 4(c1), (c2), (c3) show the real and imaginary features of noise. It can be seen from the figure that the real and imaginary parts of the ACF of noise have completely lost the real and imaginary features of the ACF of ionospheric echo and meteor echo, and most of the points are invalid data points.
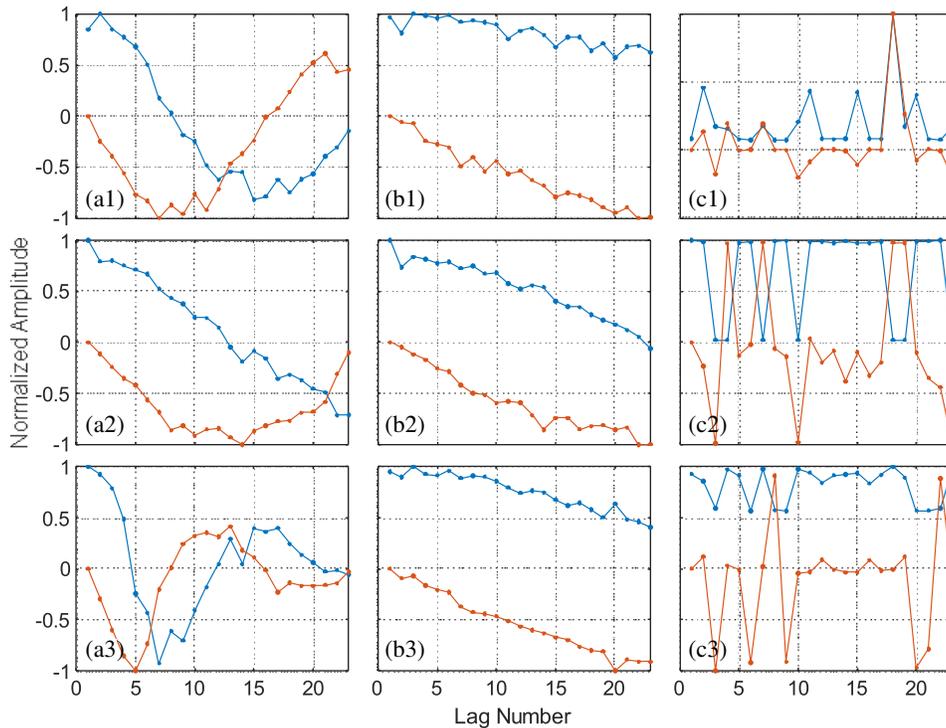

Figure 4. Real and imaginary features of AgileDARN radar echo ACF.

3. CLASSIFICATION METHOD BASED ON SVM

Support vector machine (SVM) is a machine learning algorithm for classification, regression, and estimation [27]. In the classification domain, SVM can map data to high dimensional space and transform complex classification problems into simple linear separable problems. To deal with classification problem by the concept of margin, the margin is defined as the minimum distance between the decision boundary and any samples. In the SVM, the boundary with the largest boundary is selected as the decision boundary, and the points located on the hyperplane of the maximum boundary in the feature space are called the support vector. The determination of model parameters of support vector machine is essentially a convex optimization problem [27].

SVM trains the algorithm by maximizing the separation distance between the categories. Assuming that there are N groups of data, the support vector machine is to solve the optimization problem of the following equation [28]:

$$\min \frac{1}{2}\omega^T\omega + C\sum_{i=1}^{N}\xi_i$$

$$\text{st. } d_i\left(\omega^T\phi\left(x_i\right)+b\right) \geq 1-\xi_i, \quad \xi_i \geq 0$$

(6)

where ω represents the weight, b the bias, x_i the data vector, ξ_i the relaxation factor, and C the penalty factor. Here the training vector x_i maps to a higher dimensional space with the function ϕ, and the SVM finds a linearly separable hyperplane with the largest boundary in the higher dimensional space. Generally, the penalty factor C is a parameter greater than 0, which means that some training data points are allowed to be incorrectly classified, so that the algorithm has better generalization performance. The kernel function can be expressed as $K(x_i, x_j) \equiv \phi^T(x_i)\phi(x_j)$, and the weights and biases are optimized by maximizing the boundaries.

SVM is used to classify data as follows: 1) Normalize the training data and testing data to make the data between $[-1, 1]$, so as to ensure the consistency of numerical range and avoid the feature of larger numerical value affecting the feature of smaller numerical value; 2) Since the characteristics of ionospheric echo, meteor echo, and noise are obvious and linearly separable, the linear kernel function is selected in this paper; 3) Input normalized data into SVM for training to obtain classification model; 4) Use test data to verify the classification model. The data processing flow is shown in Figure 5.
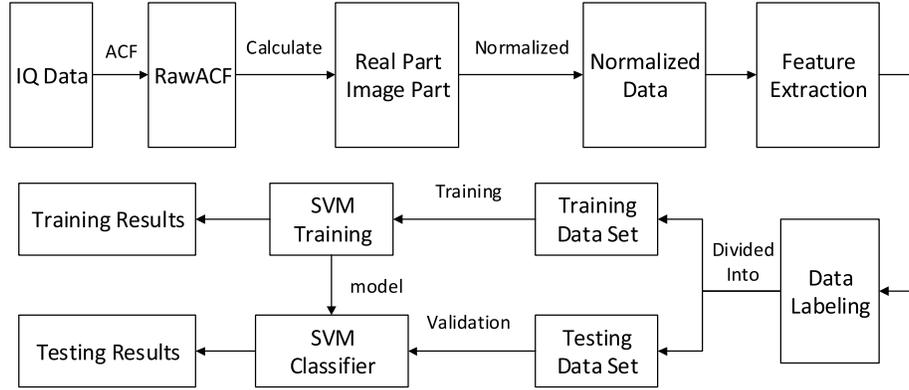

Figure 5. Data classification process flow chart based on SVM.

Figure 6. Training data set and testing data set classification results.

The real and imaginary parts of RawACF data of AgileDARN radar were incorporated into the data set. The pulse sequence of AgileDARN radar was 8 pulses with unequal intervals, and there were 23 delays after autocorrelation calculation. The data set composed of real and imaginary parts had 46 dimensional features. 2500 echoes were selected, and the noise, ionospheric echo and meteor echo were labeled as 0, 1, and 2, respectively. 60% of them were randomly selected as training data set and 40% as testing data set. In order to avoid the influence of randomness, we use the training data to train the SVM for 10 times and select the model with the highest training accuracy, so that we can obtain the best classification model of SVM.
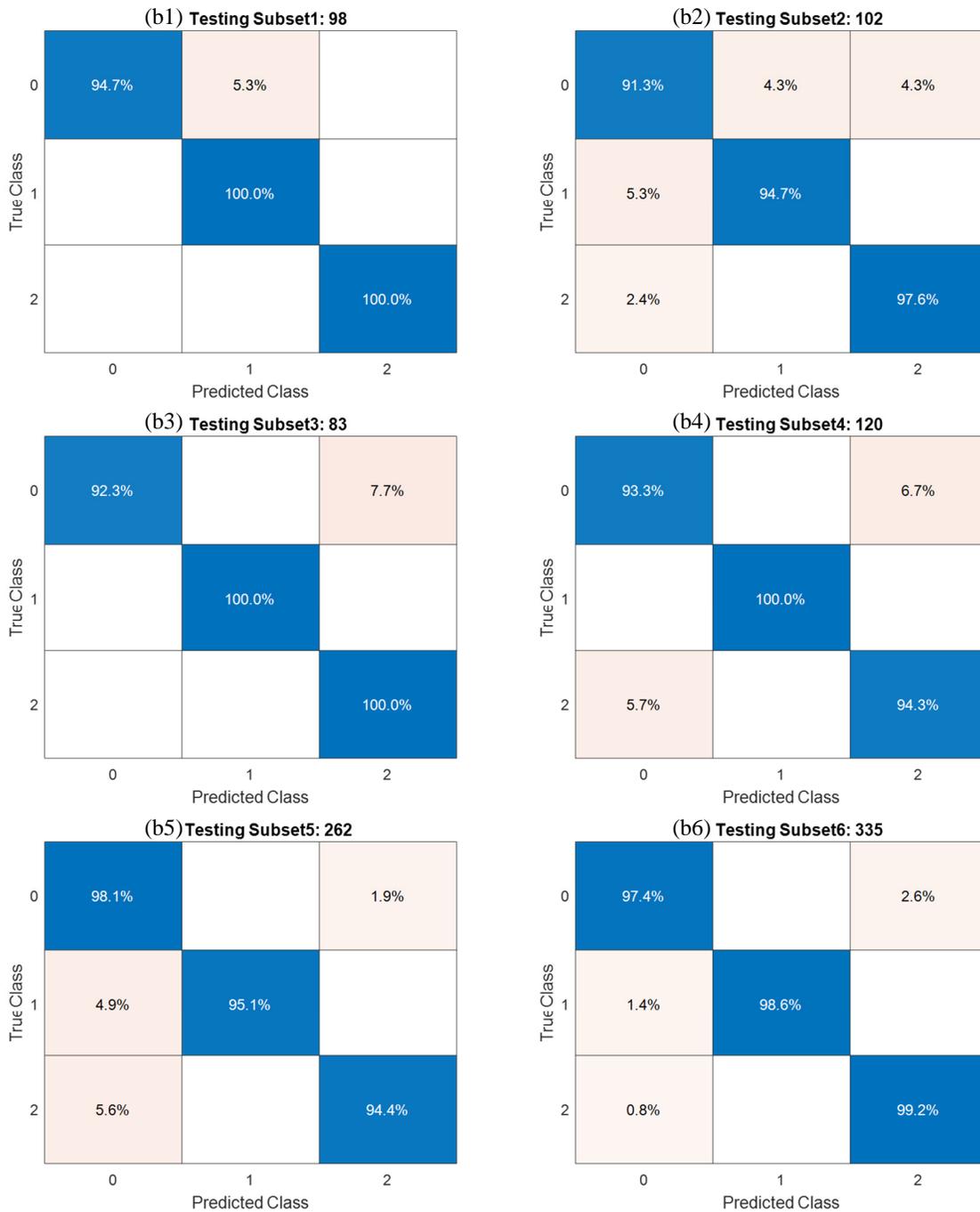

Figure 7. Classification results of each group of testing data sets.

Figures 6(a), (b) show the classification results of training data sets and testing data sets. It can be seen from Figure 6(a) that the classification accuracy of SVM is 99.5% for ionospheric echo, 99.8% for meteor echo, and 99% for noise. Figure 6(b) shows the classification results of testing data by using the trained SVM model, from which it can be seen that the classification accuracy of ionospheric echo, meteor echo, and noise is 97.6%, 97.3%, and 96%, respectively. To further verify the generalization performance of the model, the testing data were further randomly divided into 6 groups, and the confusion matrix obtained is shown in Figure 7. It can be seen from Figures 7(b1), (b2), (b3), (b4), (b5), (b6) that the classification accuracy of each group of testing data is above 91%. However, it should also be seen that a small part of noise is still identified as ionospheric echo or meteor echo, which may be due to the failure to include all possible noise data during the SVM training. The advantage of the algorithm proposed in this paper lies in the use of machine learning algorithm to automatically classify AgileDARN radar echoes and extract meteor echoes, ionospheric echoes, and noise from them.

In order to verify the actual classification performance of the algorithm in this paper for AgileDARN radar data, 1800 echo data of AgileDARN radar are classified. The confusion matrix of classification results is shown in Figure 8. As can be seen from Figure 8, the classification accuracy of ionospheric echo is 95.6%; the identification accuracy of meteor echo is 100%; and the identification accuracy of noise is 79.3%. It can be seen that the algorithm proposed in this paper can realize automatic classification of AgileDARN radar echo.
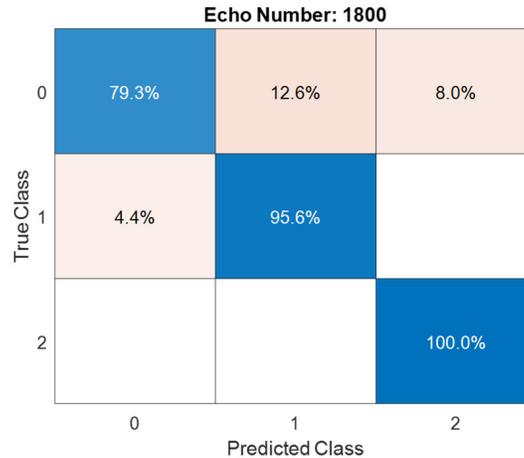
Figure 8. AgileDARN radar actual data classification results.

4. CONCLUSION

AgileDARN radar is a high-frequency radar for detecting ionospheric plasma and irregularities. In the radar echo, in addition to the ionospheric echo, there is also a meteor echo at the near range gate. In order to classify AgileDARN radar echoes and extract ionospheric and meteor echoes from them, a reliable and efficient classification method is needed for a large amount of AgileDARN radar data. Therefore, an automatic echo classification method based on support vector machine is proposed in this paper. Firstly, the calculation method of ACF is analyzed, and the characteristics of ACF of ionospheric echo, meteor echo, and noise are extracted. Then, according to the data set of the ACF of feature extracting, divided into training data and testing data sets to train and test SVM, the training data set of ionospheric echo, meteor echo, and noise of the classification accuracy is more than 99%. In order to verify the generalization performance of the algorithm, the testing data were randomly divided into 6 groups. The classification accuracy of ionospheric echo, meteor echo, and noise is more than 91%, showing good classification accuracy and generalization performance. Finally, in order to verify the performance of the algorithm, 1800 echo data of AgileDARN radar are classified. Compared with manual interpretation, the classification accuracy of ionospheric echo is 95.6%; 4.4% meteor echo is still wrongly classified as noise; the classification accuracy of meteor echo is 100%; and the classification

accuracy of noise is 79.3%. Among them, 12.6% of the noise was incorrectly classified as ionospheric echo, and 8% of the noise was incorrectly classified as ionospheric echo. To further improve the classification accuracy, one possible method is to add a recall option. Echoes that are difficult to classify are selected from the dataset, which allows large data sets to be divided into smaller data sets. It is easier to classify small data sets using a set of support vector machine classification methods with different weights and biases, which can further improve the classification accuracy.

REFERENCES

1. Greenwald, R. A., K. B. Baker, J. R. Dudeney, et al., "Darn superdarn — A global view of the dynamics of high-latitude convection," *Space Science Reviews*, Vol. 71, Nos. 1–4, 761–796, 1995.
2. Ribeiro, A. J., J. M. Ruohoniemi, P. V. Ponomarenko, et al., "A comparison of SuperDARN ACF fitting methods," *Radio Science*, Vol. 48, No. 3, 274–282, 2013.
3. Greenwald, R. A., J. B. Baker, R. A. Hutchins, et al., "An HF phased-array radar for studying small-scale structure in the high-latitude ionosphere," *Radio Science*, Vol. 20, 63–79, 1985.
4. Berngardt, O. I., J. M. Ruohoniemi, N. Nishitani, et al., "Attenuation of decameter wavelength sky noise during X-ray solar flares in 2013–2017 based on the observations of midlatitude HF radars," *Journal of Atmospheric and Solar-Terrestrial Physics*, Vol. 173, 1–13, 2018.
5. Ruohoniemi, J. M., R. A. Greenwald, J. P. Villain, et al., "Coherent HF radar backscatter from small-scale irregularities in the dusk sector of the subauroral ionosphere," *Journal of Geophysical Research-Space Physics*, Vol. 93, No. A11, 12871–12882, 1988.
6. Milan, S. E., T. K. Yeoman, M. Lester, et al., "Initial backscatter occurrence statistics from the CUTLASS HF radars," *Annales Geophysicae-Atmospheres Hydrospheres and Space Sciences*, Vol. 15, No. 6, 703–718, 1997.
7. Hall, G. E., J. W. MacDougall, D. R. Moorcroft, et al., "Super dual auroral radar network observations of meteor echoes," *Journal of Geophysical Research-Space Physics*, Vol. 102, No. A7, 14603–14614, 1997.
8. Hussey, G. C., C. E. Meek, D. Andre, et al., "A comparison of Northern Hemisphere winds using SuperDARN meteor trail and MF radar wind measurements," *Journal of Geophysical Research-Atmospheres*, Vol. 105, No. D14, 18053–18066, 2000.
9. Hibbins, R. E., M. P. Freeman, S. E. Milan, and J. M. Ruohoniemi, "Winds and tides in the mid-latitude Southern Hemisphere upper mesosphere recorded with the Falkland Islands SuperDARN radar," *Annales Geophysicae*, Vol. 29, No. 11, 1985–1996, 2011.
10. Baker, K. B. and R. A. Greenwald, "The vertical angle of arrival of highfrequency signals propagating from thule to goose bay," *Johns Hopkins APL Technical Digest*, Vol. 9, No. 2, 121–130, 1988.
11. Chisham, G. and M. Pinnock, "Assessing the contamination of SuperDARN global convection maps by non-F-region backscatter," *Annales Geophysicae*, Vol. 20, No. 1, 13–28, 2002.
12. André, R., M. Pinnock, J. P. Villain, and C. Hanuise, "Influence of magnetospheric processes on winter HF radar spectra characteristics," *Annales Geophysicae*, Vol. 20, No. 11, 1783–1793, 2002.
13. Blanchard, G. T., S. Sundeen, and K. B. Baker, "Probabilistic identification of high-frequency radar backscatter from the ground and ionosphere based on spectral characteristics," *Radio Science*, Vol. 44, No. 5, 1–9, 2009.
14. Berngardt, O. I., A. L. Voronov, and K. V. Grkovich, "Optimal signals of Golomb ruler class for spectral measurements at EKB SuperDARN radar: Theory and experiment," *Radio Science*, Vol. 50, No. 6, 486–500, 2015.
15. Barthes, L., R. André, J. C. Cerisier, and J.-P. Villain, "Separation of multiple echoes using a high-resolution spectral analysis for SuperDARN HF radars," *Radio Science*, Vol. 33, No. 4, 1005–1017, 1998.
16. Liu, E. X., H. Q. Hu, R. Y. Liu, et al., "An adjusted location model for SuperDARN backscatter echoes," *Annales Geophysicae*, Vol. 30, No. 12, 1769–1779, 2012.

17. Ribeiro, A. J., J. M. Ruohoniemi, J. B. H. Baker, et al., "A new approach for identifying ionospheric backscatter in midlatitude SuperDARN HF radar observations," *Radio Science*, Vol. 46, No. 4, 2011.

18. Lavygin, I. A., V. P. Lebedev, K. V. Grkovich, et al., "Identifying ground scatter and ionospheric scatter signals by using their fine structure at Ekaterinburg decameter coherent radar," Cornell University Library, Ithaca, 2018.

19. Matthews, D. M., M. L. Parkinson, P. L. Dyson, et al., "Optimising estimates of mesospheric neutral wind using the TIGER SuperDARN radar," *Advances in Space Research*, Vol. 38, No. 11, 2353–2360, 2006.

20. Yukimatu, A. S. and M. Tsutsumi, "A new SuperDARN meteor wind measurement: Raw time series analysis method and its application to mesopause region dynamics," *Geophysical Research Letters*, Vol. 29, No. 20, 2002.

21. Tsutsumi, M., A. S. Yukimatu, D. A. Holdsworth, et al., "Advanced SuperDARN meteor wind observations based on raw time series analysis technique," *Radio Science*, Vol. 44, No. 2, 1–11, 2009.

22. Parris, R. T., "Design and implementation of a meteor tracking retrofit system for the HF radar at Kodiak Island, Alaska," 110, University of Alaska Fairbanks, Ann Arbor, 2003.

23. Song, J., A. L. Lan, J. Y. Yan, et al., "Analysis of FPGA implementation for AgileDARN radar digital system," *Remote Sensing Technology and Application*, Vol. 32, No. 6, 1064–1070, 2017.

24. Farley, D. T., "Multiple-pulse incoherent-scatter correlation function measurements," *Radio Science*, Vol. 7, No. 6, 661–666, 1972.

25. Hanuise, C., R. A. Greenwald, and K. B. Baker, "Drift motions of very high latitude F region irregularities: Azimuthal Doppler analysis," *Journal of Geophysical Research*, Vol. 90, No. A10, 1985.

26. Baker, J. B., R. A. Greenwald, J. P. Villain, et al., "spectral characteristics of high frequency backscatter from high latitude ionospheric irregularities — Preliminary analysis of statistical properties," *Interim Rep.*, RADC-TR-87-284, Rome Air Dev. Cent., Briffis Air Force Base, 1988.

27. Cristianini, J. S.-T. N., *An Introduction to Support Vector Machines and Other Kernel-based Learning Methods*, Cambridge University Press, 2000.

28. Burges, C. J., "A tutorial on support vector machines for pattern recognition," *Data Mining Knowledge Discovery*, 1998.